Final Report For U.S. DEPARTMENT OF ENERGY GRANT: DE-FG02-00ER14980

To: Raul Miranda, Chemical Sciences, Geosciences and Biosciences Division, Office of Basic Energy Sciences

Title: Synthesis and Characterization of Cluster-Derived Supported Bimetallic Catalysts

Richard D. Adams, PI[1]
Michael D. Amiridis, Co-PI[2]

[1]Department of Chemistry and Biochemistry
University of South Carolina
Columbia, SC 29208

[2]Department of Chemical Engineering
University of South Carolina
Columbia, SC 29208

October 2008

Executive Summary

New procedures have been developed for synthesizing di- and tri-metallic cluster complexes. The chemical properties of the new complexes have been investigated, particularly toward the activation of molecular hydrogen. These complexes were then converted into bi- and tri-metallic nanoparticles on silica and alumina supports. These nanoparticles were characterized by electron microscopy and were then tested for their ability to produce catalytic hydrogenation of unsaturated hydrocarbons and for the preferential oxidation of CO in the presence of hydrogen. The bi- and tri-metallic nanoparticles exhibited far superior activity and selectivity as hydrogenation catalysts when compared to the individual metallic components. It was found that the addition of tin greatly improved the selectivity of the catalysts for the hydrogenation of polyolefins. The addition of iron improves the catalysts for the selective oxidation of CO by platinum in the presence of hydrogen. The observations should lead to the development of lower cost routes to molecules that can be used to produce polymers and plastics for use by the general public and for procedures to purify hydrogen for use as an alternative energy in the hydrogen economy of the future.

Comparison of Accomplishments with Goals and Objectives of the project.

The objectives of the project were to provide new bimetallic cluster complexes and convert these into useful catalysts. These objectives were met and the superior activity of the new catalysts exceeded the goals of the project.

Summary of Project Activities 2005 – 2008

Contents

A) Richard Adams Research Results.

1) Unsaturated Bimetallic Platinum-Rhenium Cluster Complexes that Activate Hydrogen under Mild Conditions
2) New Platinum Bimetallic cluster Complexes Containing Rhodium
3) New Palladium Bimetallic cluster Complexes Containing Ruthenium
4) New Platinum and Palladium Cluster Complexes Containing Osmium
5) High Nuclearity Bimetallic Platinum-Iridium Cluster Complexes
6) Rhodium and Iridium Cluster Complexes Containing Unusually Large Numbers of Phenyl Tin Ligands
7) New Rhenium and Ruthenium Cluster Complexes Containing Diphenyltin and Diphenylgermanium Ligands that add Platinum and Palladium to the Re-Sn, Re-Ge and Ru - Sn Bonds
8) Synthesis of Trimetallic cluster complexes by the addition of Diphenyltin and Diphenylgermanium Ligands to Platinum-Ruthenium Cluster complexes
9) New Highly Active Tin- Containing NanoCatalysts for the Selective Hydrogenations
    a) The Hydrogenation of Dimethylterephthalate by using a Platinum-Ruthenium-Tin Precursor Complex.
    b) Selective Catalysts for the Hydrogenation of Cyclododecatriene

B) Michael Amiridis Research Results

1) Pt_4 clusters in aqueous solutions as precursors for heterogeneous catalysts
2) Structure and reactivity of cluster-derived $PtFe/SiO_2$ catalysts
3) Investigation of $PtFe/SiO_2$ catalysts prepared by coimpregnation
4) Kinetic characterization of multimetallic cluster-derived catalysts

C) Publications for this Project for the Years 2005 - 2008.

1) Richard D. Adams Publications
2) Michael D. Amiridis Publications

A) Richard Adams Results 2005-2008.

Details of all of our published results can be found in the 40 publications listed under Richard D. Adams at the end of this section of the report. Highlights of our results are summarized in the following sections.

1) Unsaturated Bimetallic Platinum-Rhenium Cluster Complexes that Activate Hydrogen under Mild Conditions

There has been much interest in the activation of hydrogen by metal complexes in recent years. Complexes that can make multiple additions of hydrogen are being actively sought. In this work, we have taken advantage of the beneficial effects of highly sterically encumbered phosphine ligands, such as PBu^t_3, to synthesize new electronically unsaturated polynuclear metal cluster complexes. During this project, we have prepared a number of new highly unsaturated bimetallic platinum-rhenium carbonyl cluster complexes that are capable of multiple additions of hydrogen. In some cases, these additions are even ***reversible***.

1) The reaction of $Re_2(CO)_{10}$ with $Pt(PtBu_3)_2$ has yielded the new unsaturated platinum-rhenium cluster complex $Pt_3Re_2(CO)_6(PtBu_3)_3$, **1**, see Figure 1. Compound **1** contains a trigonal bipyramidal cluster of five metal atoms with the three platinum atoms in the equatorial plane and the two rhenium atoms in the apical positions. The compound is electronically unsaturated by the amount of ***10*** valence electrons. Compound **1** reacts with hydrogen at room temperature to relieve this unsaturation by adding three equivalents of H_2 to form the hexahydrido cluster complex $Pt_3Re_2(CO)_6(PtBu_3)_3(\mu\text{-}H)_6$, **2** in 90 % yield, see Figure 2. The metal cluster in **2** has a trigonal bipyramidal structure similar to that of **1**, but it also contains six bridging hydrido ligands one on each of the six Re-Pt bonds in the complex. The electronic structure of **1** was investigated by Fenske-Hall molecular orbital calculations which revealed the nature of the low lying empty orbitals and showed which ones were filled with electrons when the hydrogen was added to it.

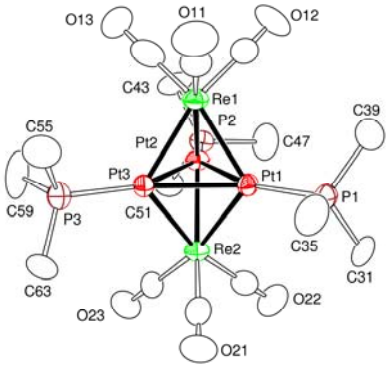

Figure 1. ORTEP diagram of **1**.

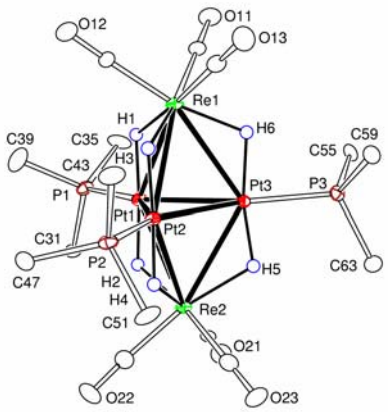

Figure 2. ORTEP diagram of **2**.

From the reaction of $Pt(PtBu_3)_2$ with $Re_3(CO)_{12}(\mu\text{-}H)_3$, two new compounds $PtRe_2(CO)_9(PtBu_3)(\mu\text{-}H)_2$, **3** and $Pt_2Re_2(CO)_7(PtBu_3)_2(\mu\text{-}H)_2$, **4** were obtained. Compound **3**

contains a triangular $PtRe_2$ cluster with two bridging hydrido ligands. Compound **4** is a highly electron deficient (54 valence electrons) that contains a tetrahedrally shaped Pt_2Re_2 cluster with two bridging hydrido ligands, see Figure 3, that are dynamically averaged on the ^1H NMR time scale at room temperature. Compound **4** was found to add one equivalent of hydrogen at 25° C (1 atm) to yield the new tetrahydrido complex $Pt_2Re_2(CO)_7(PtBu_3)_2(\mu\text{-}H)_4$, **5**, see Figure 4. Compound **4** contains four hydrido ligands: one terminal, two edge bridging and one triple bridge. Most interestingly, the addition of hydrogen to **3** was shown to be reversible, when heated to 97° C, **5** is converted back to **4** by loss of H_2 in 90% isolated yield. Compound **5** also eliminates hydrogen to regenerate **4** when irradiated (UV-vis) at room temperature. Because of their superior properties, heterogeneous platinum-rhenium nanoparticle catalysts are widely used by the petroleum industry for the process known as reforming.

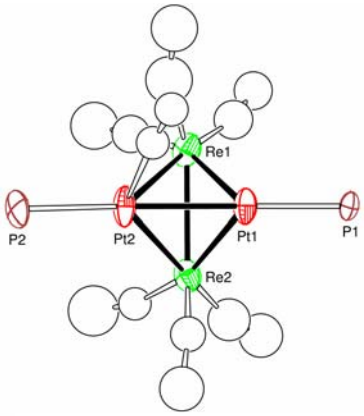

Figure 3. ORTEP diagram of **4**. Hydride ligands not shown.

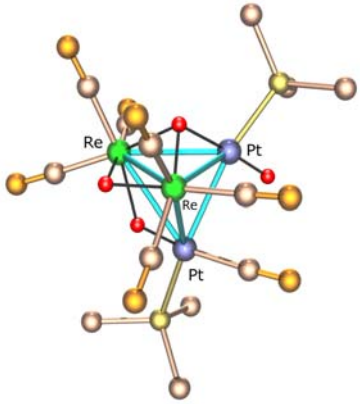

Figure 4. Structural diagram of **5**. Hydride ligands are shown in red.

2) New Platinum Bimetallic Cluster Complexes Containing Rhodium.

Platinum-rhodium bimetallic catalysts are widely used in automotive catalytic converters to remove exhaust pollutants. In hopes of using bimetallic platinum-rhodium cluster complexes as catalyst precursors, we have prepared a number of new platinum-rhodium cluster complexes and have investigated their structures and properties. The reaction of $Rh_4(CO)_{12}$ with $Pt(PBu^t_3)_2$ in CH_2Cl_2 at room temperature yielded three new complexes: $Rh_4(CO)_4(\mu\text{-}CO)_4(\mu_4\text{-}CO)(PBu^t_3)_2[Pt(PBu^t_3)]$, **6**, $Rh_2(CO)_8[Pt(PBu^t_3)]_2[Pt(CO)]$, **7** and $Rh_2(CO)_8[Pt(PBu^t_3)]_3$, **8**. The reaction of $Rh_4(CO)_{12}$ with an excess of $Pt(PBu^t_3)_2$ in hexane at 68° C yielded the new hexarhodium-tetraplatinum compound, $Rh_6(CO)_{16}[Pt(PBu^t_3)]_4$, **9**. All four compounds were characterized by ^{31}P NMR and single crystal X-ray diffraction analyses. Compound **6** contains an unsymmetrical quadruply bridging carbonyl ligand in the fold of a butterfly tetrahedral cluster of four rhodium atoms with a $Pt(PBu^t_3)$ group bridging the hinge of the butterfly tetrahedron. Compound **7** contains an unsaturated trigonal bipyramidal Rh_2Pt_3 cluster. Compound **8** is similar to **7** except the trigonal bipyramidal Rh_2Pt_3 cluster opened by cleavage of one Pt-Rh bond due to steric interactions produced by the replacement of one of the carbonyl ligands in **7** with a tri-t-butylphosphine ligand. Compound **8** undergoes facile dynamical rearrangements of the metal atoms in the cluster which average the three inequivalent phosphine ligands on the platinum atoms. Compound **9** contains an octahedral cluster of six rhodium atoms with four $Pt(PBu^t_3)$ groups bridging edges of that octahedron.

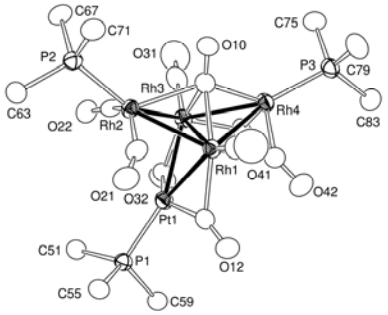

Compound **6**

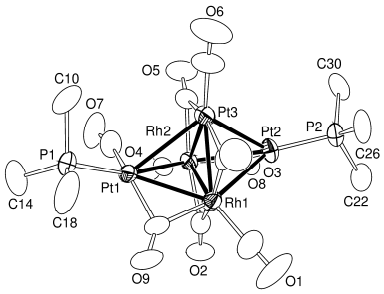

Compound **7**

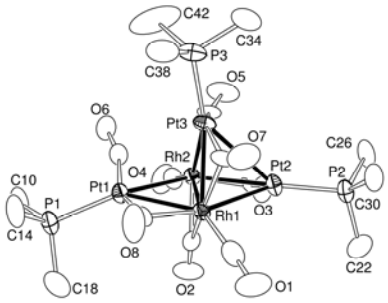

Compound **8**

3) New Platinum and Palladium Bimetallic Cluster Complexes Containing Ruthenium

We have discovered that the complex $Pd(PBu^t_3)_2$ reacts with ruthenium carbonyl complexes to introduce a $Pd(PBu^t_3)$ fragment across ruthenium – ruthenium bonds to synthesize new series of new bimetallic palladium-ruthenium cluster complexes. Palladium-ruthenium complexes have been shown to be precursors to good bimetallic catalysts on supports. For example, the reaction of $Pd(PBu^t_3)_2$ with $Ru_3(CO)_{12}$ yielded the unusual tripalladium adduct $Ru_3(CO)_{12}[Pd(PBu^t_3)]_3$ **10** of $Ru_3(CO)_{12}$, see Figure 5. Compound **10** contains three $Pd(PBu^t_3)$ groups symmetrically disposed with each one acting as a bridge across one Ru–Ru bond of the former $Ru_3(CO)_{12}$ molecule. Compound **10** is electron deficient too. With the help of Professor Michael Hall at Texas A&M University, the nature of the unsaturation in the metal – metal bonds has been revealed. Figure 6 shows one of three identical 3 center – 2 electron bonds that form the basis of the metal – metal bonding in **10**. The platinum containing homologue of **10** was also prepared and studied.

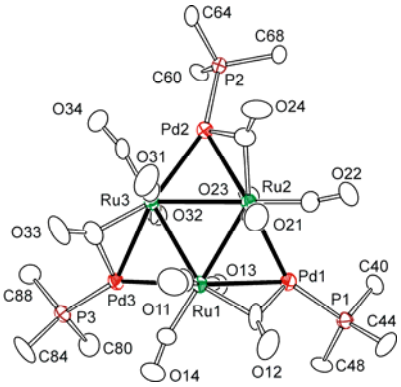

Figure 5. An ORTEP diagram of **10**.

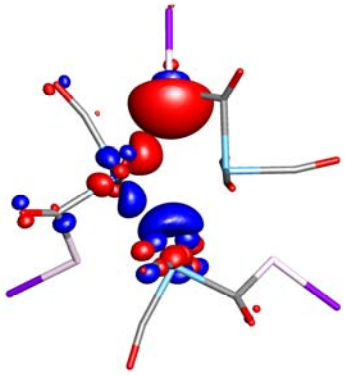

Figure 6. Molecular Orbital diagram of **10**.

4) New Platinum and Palladium Cluster Complexes Containing Osmium

From the reaction of $Pt(PBu^t_3)_2$ with $Os_3(CO)_{12}$ at room temperature, we have obtained the complete series of the three compounds $PtOs_3(CO)_{12}(PBu^t_3)$, **11**, $Pt_2Os_3(CO)_{12}(PBu^t_3)_2$, **12** and $Pt_3Os_3(CO)_{12}(PBu^t_3)_3$, **13** involving the sequential addition of one through three $Pt(PBu^t_3)$ groups to the three Os – Os bonds of the metal cluster of $Os_3(CO)_{12}$. Compound **13** is structurally similar to **10**. In solution compounds **11** – **13** interconvert among themselves by *intermolecular* exchange of the $Pt(PBu^t_3)$ groups, see Scheme 1. When **12** is treated with PPh_3 at room temperature, the mono and bis-PPh_3 derivatives of $Os_3(CO)_{12}$, $Os_3(CO)_{11}(PPh_3)$ and

$Os_3(CO)_{10}(PPh_3)_2$ were obtained by elimination of the $Pt(PBu^t_3)$ groups together with one and two CO ligands, respectively. These compounds can be obtained from $Os_3(CO)_{12}$ with PPh_3 only by heating to 140° C. Our work shows that the $Pt(PBu^t_3)$ groups assist and facilitate the CO ligand substitution in **12**. We have also made and structurally characterized the Pd homologs of **12** and **13**.

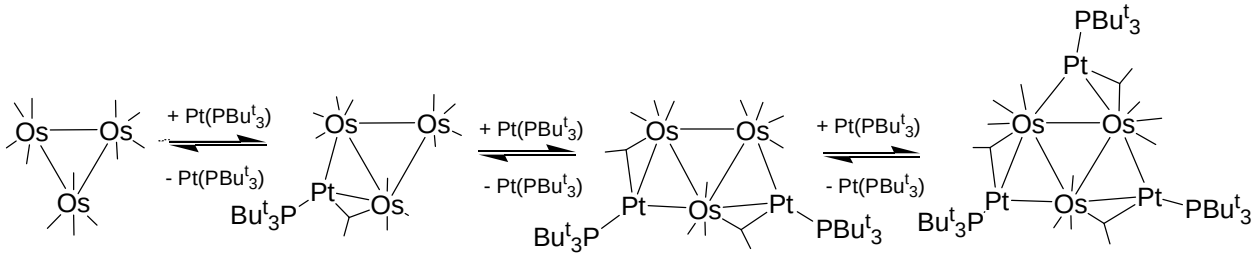

11 **12** **13**

Scheme 1

At higher temperatures the Os_3 cluster grew into a tetrahedral Os_4 cluster that added four $Pd(PBu^t_3)$ groups to yield the eight metal cluster complex $Os_4(CO)_{12}[\mu_3\text{-}Pd(PBu^t_3)]_4$, **14** that contained four triply bridging $Pd(PBu^t_3)$ groups, one each of the four faces of the Os_4 tetrahedron.

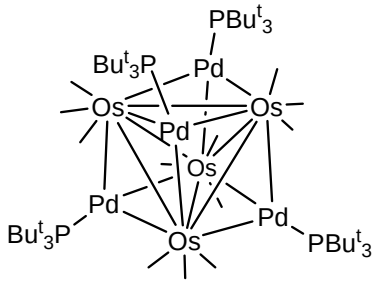

14

It was not possible to prepare the platinum homologue of **14** from the reaction of $Os_3(CO)_{12}$ with $Pt(PBu^t_3)_2$, but an interesting triosmium complex, $Os_3(CO)_{10}[Pt(PBu^t_3)]_2$, **15** with two triply-bridging $Pt(PBu^t_3)$ groups was obtained from the reaction of $Os_3(CO)_{10}(NCMe)_2$ with $Pt(PBu^t_3)_2$. Most interestingly, compound **15** was found to react readily with hydrogen even at 0° C. Two products were formed in a sequence of two H_2 additions to yield the compounds $Os_3(CO)_{10}[Pt(PBu^t_3)]_2(\mu\text{-}H)_2$, **16** and $Os_3(CO)_{10}[Pt(PBu^t_3)]_2(\mu\text{-}H)_4$, **17**, eq. (1).

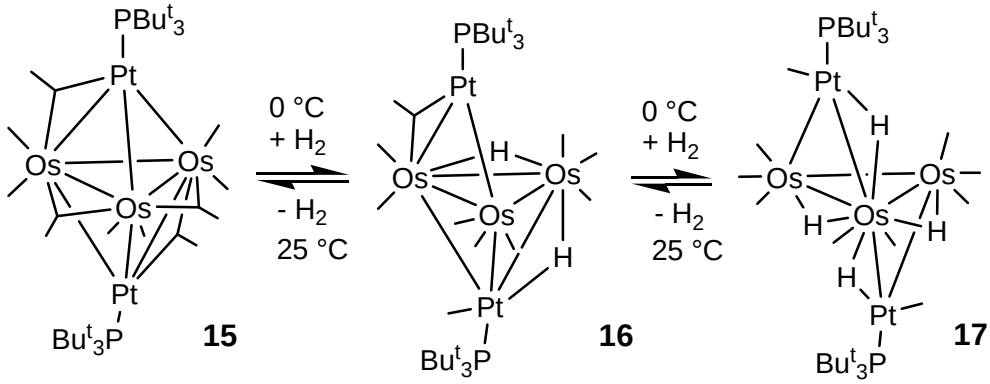

15 **16** **17** (1)

With each addition of H_2 one Pt – Os bond was cleaved and one of the triply-bridging $Pt(PBu^t_3)$ groups was converted to an edge-bridging group and a CO ligand was shifted to a terminal position on the platinum atom. The hydrogen was converted to hydrido ligands that bridge metal – metal bonds. The product **17**, thus, contains two bridging $Pt(PBu^t_3)(CO)$ groups and four bridging hydrido ligands. The H_2 activation process of compound **15** is fundamentally different from that of the previously described compounds because metal – metal bond cleavages are involved. The reason for this can be attributed to it electronic configuration. Compound **15** is only slightly electron deficient, 68 valence electrons versus the expected 72 electron count. In fact, one could argue that **15** is not unsaturated at all if one accepts 16 electron configurations for the two platinum atoms as the norm. Thus, the electrons that are added to the cluster of **15**, upon addition of H_2, do not go into empty molecular orbitals, but instead go into antibonding orbitals that ultimately lead to the cleavages of metal – metal bonds the subsequent structural rearrangements. Interestingly, addition of hydrogen to **15** is readily reversible; simple purging of solutions of **16** and **17** with nitrogen regenerates **15**. The problem with this reaction is that **17** continues to react with hydrogen with time and this results in irreversible degradation of the complex by loss of a platinum containing group.

Perhaps one of the more stunning examples of bond activation by the $Pt(PBu^t_3)$ group is the activation of the M – H bond in the complexes, $HM(CO)_4(SnPh_3)$, **18** - **19**, M = Ru and Os toward alkyne insertion. Complex **18** does not react with PhC_2H even in a toluene solution at reflux (110° C). However, solutions of **19** and PhC_2H containing $Pt(PBu^t_3)_2$ react rapidly to yield the mixed metal complex $PtOs(CO)_4(SnPh_3)(PBu^t_3)[\mu\text{-}HCC(H)Ph]$, **20** which contains a HCC(H)Ph ligand bridging the Pt – Os bond in this dinuclear metal complex. The HCC(H)Ph ligand was formed by insertion of the PhC_2H into the Os – H bond and transfer of the hydrogen atom to the phenyl-substituted carbon atom. To understand this complex reaction, the reaction of $Pt(PBu^t_3)_2$ with **19** was investigated in the absence of PhC_2H. This reaction produced the platinum-osmium complex $PtOs(CO)_4(SnPh_3)(PBu^t_3)(\mu\text{-}H)$, **21** which was subsequently found to be the precursor to **20**. The molecular structure of **21** is shown in Figure 7.

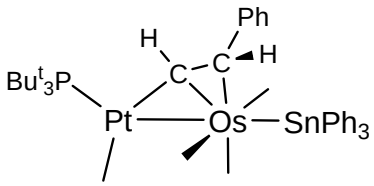

20

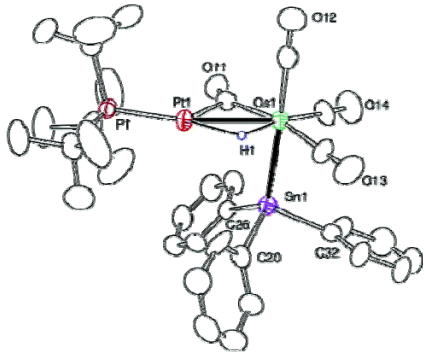

Figure 7. An ORTEP diagram of the molecular structure of **21**.

Although it contains a metal – metal bond, a bridging hydrido ligand and a bridging carbonyl ligand, compound **21** can still be viewed as a $Pt(PBu^t_3)$ adduct of **19**. Compound **21** reacts with PhC_2H to give **20**. From the structure of **21** one can immediately see how the platinum atom activates the Os – H bond. It has formed a bonding interaction to both the osmium and the

hydrogen atom. The Os – H bond length in **21**, Os(1)-H(1) = 1.95(6) Å, is substantially longer than that in **19**, 1.67(4) Å.

A molecular orbital analysis of **21** provided some additional insight into the nature of the reaction of the **21** with PhC_2H and the role of the platinum atom in particular. A contour diagram of the lowest unoccupied molecular orbital (LUMO) of **21** is shown in Figure 8. An obvious feature of this orbital is that it contains a large component on the platinum atom. It is believed that this frontier orbital is the one that facilitates the addition of the PhC_2H molecule to **21** via formation of a bonding interaction between the platinum atom and the π–bond of the PhC_2H molecule, and in turn, because of its proximity and interaction with the hydrido ligand, it also promotes the insertion of the PhC_2H ligand into the Pt – H and Os – H bonds.

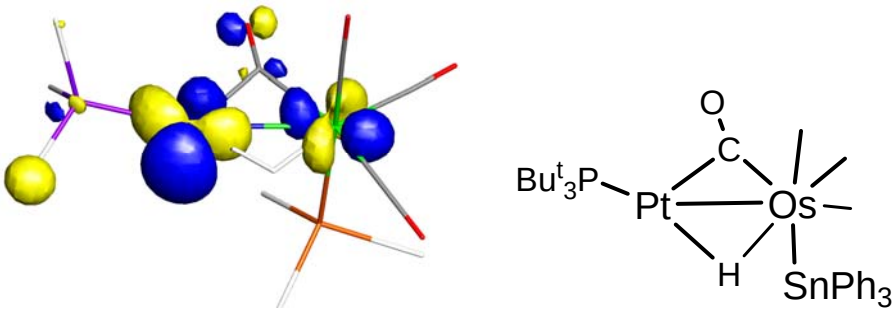

Figure 8. A contour diagram of the Fenske-Hall LUMO of **21** and a line structure (right) showing the orientation of the atoms in the contour diagram.

5) High Nuclearity Bimetallic Platinum-Iridium Cluster Complexes

In his pioneering work on petroleum reforming catalysts, J. Sinfelt showed that when platinum was combined with iridium, a vastly superior catalyst was produced. Today, bimetallic reforming catalysts are in widespread use industrially. Bimetallic catalysts have an advantage over their monometallic counterparts both in higher activity and higher selectivity due to synergy between the different elements. Bimetallic metal clusters have been shown to be excellent precursors to heterogeneous bimetallic catalysts when placed on supports. During this grant period we have investigated the reaction of $Ir_4(CO)_{12}$ with $Pt(PBu^t_3)_2$. From these reagents we have prepared the highest nuclearity platinum-iridium cluster complexes reported to date.

At room temperature the reagents combine to form a very simple bis-$Pt(PBu^t_3)$ adduct of $Ir_4(CO)_{12}$, $Ir_4(CO)_{12}[Pt(PBu^t_3)]_2$, **22**, which contains $Pt(PBu^t_3)$ groups bridging opposite edges of a central Ir_4 pseudo-tetrahedron. However, the same reaction at 110 ºC yielded two higher nuclearity complexes, $Ir_8(CO)_{12}[Pt(PBu^t_3)]_4$, **23** and $Ir_6(CO)_{10}[Pt(PBu^t_3)]_4$, **24**. Compound **23** consists of a central $Ir_4(CO)_4$ tetrahedron with four edge-bridging $Ir(CO)_2$ groups and four $Pt(PBu^t_3)$ groups that are each bonded to Ir_3 triangles of the Ir_4 tetrahedron and two of the $Ir(CO)_2$ groups, see Figure 9. Compound **24** consists of a central $Ir_4(CO)_4$ pseudo-tetrahedron with two edge-bridging $Ir(CO)_2$ groups and four $Pt(PBu^t_3)$ groups: one $Pt(PBu^t_3)$ group is bonded to five iridium atoms as found in **23**, two are bonded to four iridium atoms and one is bonded to one of the outer Ir_2Pt triangles, see Figure 10. Compound **24** reacts with hydrogen at 97 ºC to give the new tetra-hydrido complex $Ir_6(CO)_8[Pt(PBu^t_3)]_4(\mu\text{-}H)_4$, **25**, see Figure 11. Compound **25** is formed by the loss of the two bridging carbonyl ligands from **24** and the addition of two equivalents of hydrogen for form four bridging hydrido ligands. The bonding in **22** was

evaluated by Fenske-Hall molecular orbital calculations to help to develop and deeper understanding of the delocalized nature of the Ir-Ir and Ir-Pt bonding.

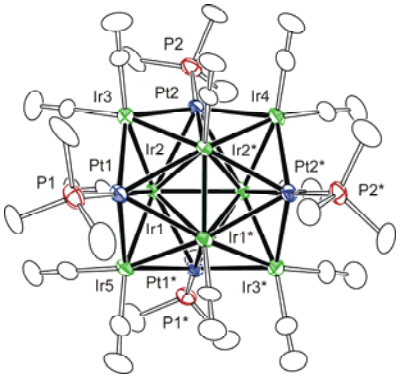

Figure 9. An ORTEP diagram of **23**.

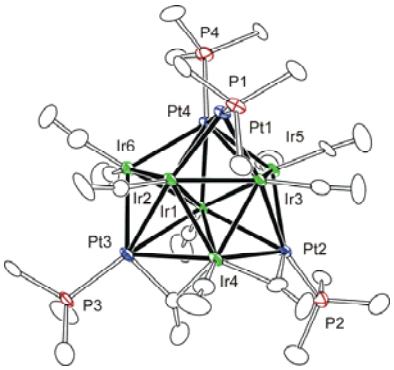

Figure 10. An ORTEP diagram of **24**.

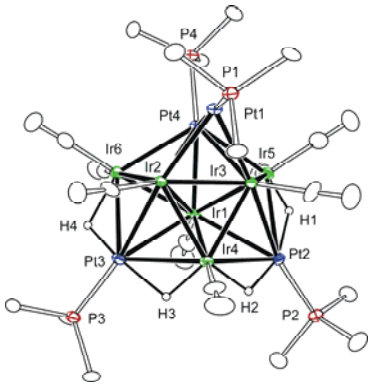

Figure 11. An ORTEP diagram of **25**.

6) Rhodium and Iridium Cluster Complexes Containing Unusually Large Numbers of Phenyl Tin Ligands

Tin is widely used as a modifier for transition metal catalysts to improve their product selectivities. In previous work we showed that Ph_3SnH will add to Ru_5 carbonyl clusters by elimination of benzene to yield Ru_5 clusters containing large numbers of bridging $SnPh_2$ ligands. During this grant period, we have extended these studies to include rhodium and iridium, and rhenium (see next section). The reactions of $Rh_4(CO)_{12}$ and $Ir_4(CO)_{12}$ with Ph_3SnH have yielded the new complexes $M_3(CO)_6(\mu\text{-}SnPh_2)_3(SnPh_3)_3$, **26** (M = Rh) and **27** (M = Ir), that contain triangular M_3 clusters with three bridging $SnPh_2$ and three terminal $SnPh_3$ ligands, see Figure 10. The Rh-Rh bond distances are unusually long. Molecular orbital calculations of **18** have shown that the cluster is stabilized by strong Rh-Sn bonding and the direct Rh-Rh interactions are weak, as shown in the symmetric HOMO in Figure 12. Reaction of **26** with Ph_3SnH yielded the complex $Rh_3(CO)_3(SnPh_3)_3(\mu\text{-}SnPh_2)_3(\mu_3\text{-}SnPh)_2$, **28**, that contains an amazing eight phenyltin ligands including the first examples of triply bridging SnPh ligands found in any transition metal cluster complex, see Figure 14.

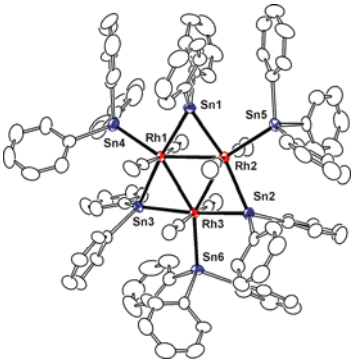

Figure 12. An ORTEP diagram of **26**.

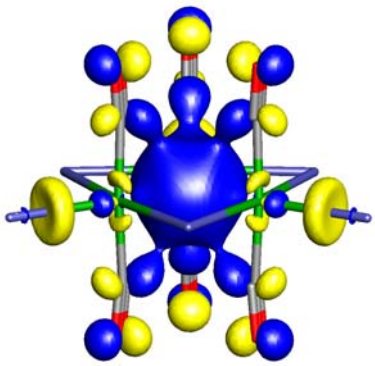

Figure 13. Diagram of the Highest Occupied Molecular Orbital in **26**.

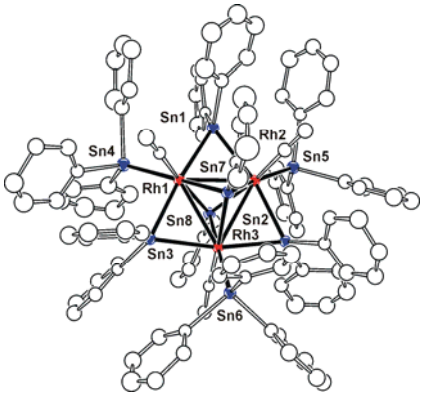

Figure 14. An ORTEP diagram of **28**.

7) New Rhenium and Ruthenium Cluster Complexes Containing Diphenyltin and Diphenylgermanium Ligands that add Platinum and Palladium to the Re-Sn, Re-Ge and Ru - Sn Bonds

Reaction of $Re_2(CO)_8[\mu\text{-}\eta^4\text{-}C(H)=C(H)Bu^n](\mu\text{-}H)$ with Ph_3SnH yielded the new compound $Re_2(CO)_8(\mu\text{-}SnPh_2)_2$, **29** that contains two $SnPh_2$ ligands bridging two $Re(CO)_4$ groups, see Figure 15. The analogous germanium compound $Re_2(CO)_8(\mu\text{-}GePh_2)_2$, **30** was obtained similarly from the reaction of $Re_2(CO)_8[\mu\text{-}\eta^4\text{-}C(H)=C(H)Bu^n](\mu\text{-}H)$ with Ph_3GeH. The reaction of **29** with $Pd(PBu^t_3)_2$ yielded the bis-$Pd(PBu^t_3)$ adduct $Re_2(CO)_8(\mu\text{-}SnPh_2)_2[Pd(PBu^t_3)]_2$, **31** that contains the first examples of $Pd(PBu^t_3)$ groups bridging transition metal-tin bonds, in this first case they are Re–Sn bonds, see Figure 16. Fenske-Hall molecular orbital calculations show that the $Pd(PBu^t_3)$ groups form three-center two-electron bonds with the neighboring rhenium and tin atoms. The mono- and bis-$Pt(PBu^t_3)$ adducts, $Re_2(CO)_8(\mu\text{-}SnPh_2)_2[Pt(PBu^t_3)]$, **32** and $Re_2(CO)_8(\mu\text{-}SnPh_2)_2[Pt(PBu^t_3)]_2$, **33** were formed when **29** was treated with $Pt(PBu^t_3)_2$. A mono adduct of **30**, $Re_2(CO)_8(\mu\text{-}GePh_2)_2[Pt(PBu^t_3)]$, **26** was obtained similarly by reaction of **30** with $Pt(PBu^t_3)_2$.

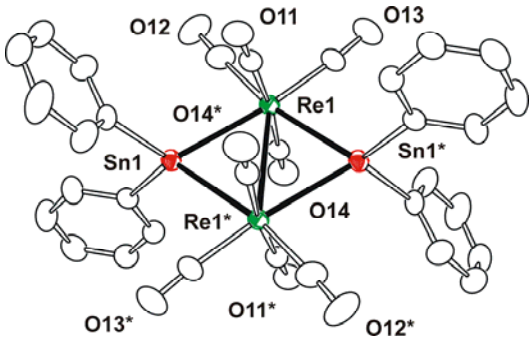

Figure 15. An ORTEP diagram of **29**.

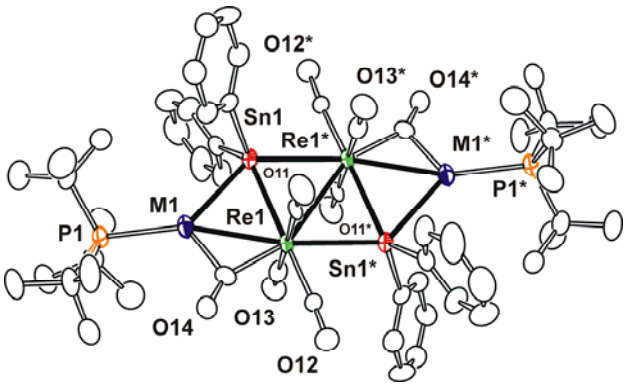

Figure 16. An ORTEP diagram of **31**, M=Pd.

We also found that mono-, bis- and tris-$Pt(PBu^t_3)$ adducts, $Ru_3(CO)_9(\mu\text{-}SnPh_2)_3[Pt(PBu^t_3)]_n$, **35** – **37**, n = 1-3, could be obtained from the reaction of the planar cluster complex $Ru_3(CO)_9(\mu\text{-}SnPh_2)_3$ with $Pt(PBu^t_3)_2$. Compounds **35** – **37** are planar and are formed by the progressive addition of 1 – 3 $Pt(PBu^t_3)$ groups to Ru – Sn bonds around the periphery of the central Ru_3Sn_3 cluster. Each addition of a $Pt(PBu^t_3)$ group destabilized the HOMO of the $Ru_3(CO)_9(\mu\text{-}SnPh_2)_3$ cluster which resulted in a progressively smaller HOMO-LUMO gap and an increasing red-shift of the principal absorption in the UV-vis absorption spectrum.

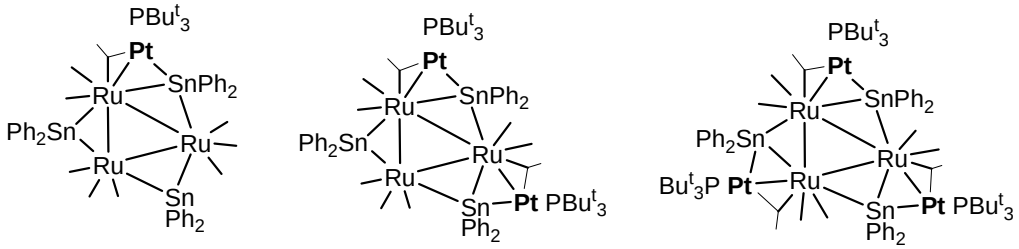

35 **36** **37**

To compare the relative affinity of the Pt(PBu$^t_3$) group for an Ru – Ru bond versus an Ru – Sn bond, the reaction of $Ru_2(CO)_8(\mu\text{-}SnPh_2)$, **38** with $Pt(PBu^t_3)_2$ was investigated. Both mono- and bis-Pt(PBu$^t_3$) adducts: $Ru_2(CO)_8(\mu\text{-}SnPh_2)[Pt(PBu^t_3)]$, **39** and $Ru_2(CO)_8(\mu\text{-}SnPh_2)[Pt(PBu^t_3)]_2$, **40** were obtained eq. (2). The structural analysis of the mono-adduct showed that the first Pt(PBu$^t_3$) group was added to the Ru – Ru bond of **38**. The second Pt(PBu$^t_3$) addition then occurred at one of the Ru – Sn bonds to yield **40**. A molecular orbital analysis of **38** provided an explanation for the preference of the Pt(PBu$^t_3$) for the Ru – Ru bond in **38** by showing that the orbital representing the Ru – Ru bond is energetically more accessible than the Ru – Sn orbitals.

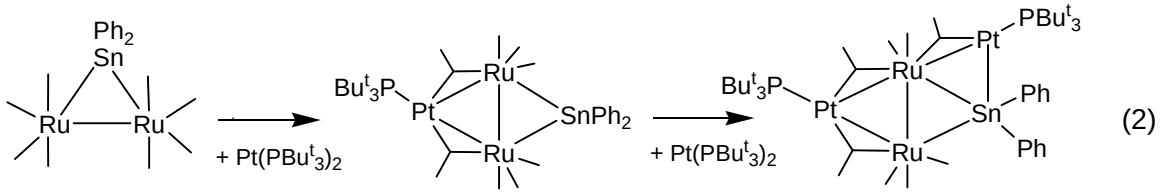

(2)

20 **21** **22**

8) Synthesis of Trimetallic cluster complexes by the addition of Diphenyltin and Diphenylgermanium Ligands to Platinum-Ruthenium Cluster complexes

Two trimetallic PtSnRu cluster complexes, $PtRu_5(CO)_{13}(PBu^t_3)(\mu\text{-}H)_3(SnPh_3)(\mu_5\text{-}C)$, **41**and $PtRu_5(CO)_{13}(PBu^t_3)(\mu\text{-}H)_2(\mu\text{-}SnPh_2)(\mu_6\text{-}C)$, **42** were obtained from the reaction of $PtRu_5(CO)_{14}(PBu^t_3)(\mu\text{-}H)_2(\mu_6\text{-}C)$, **43** with $HSnPh_3$. The first cluster complex **41** formed by a simple oxidative addition of the SnH bond of the $HSnPh_3$ to has an open structure in which the Pt(PBu$^t_3$) group bridges an edge of the square base of the square pyramidal Ru_5 cluster and contains a single $SnPh_3$ ligand. Compound **41** also has three bridging hydrido ligands and one terminal $GePh_3$ ligand. When heated to 97^o C, **41** is slowly converted to **42** by cleavage of a phenyl group from the $SnPh_3$ ligand and elimination of benzene by its combination with one of the hydrido ligands. The $PtRu_5$ metal cluster of **42** has a closed octahedral shape with an $SnPh_2$ ligand bridging one of the Ru–Ru bonds, see Figure 17. The two analogous germanium containing compounds $PtRu_5(CO)_{13}(PBu^t_3)(\mu\text{-}$

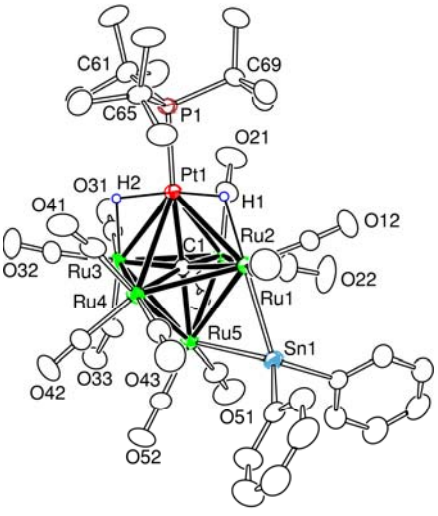

Figure 17. An ORTEP diagram of **41**.

$H)_3(SnPh_3)(\mu_5\text{-}C)$ and $PtRu_5(CO)_{13}(PBu^t_3)(\mu\text{-}H)_2(\mu\text{-}SnPh_2)(\mu_6\text{-}C)$, which are analogous to **41** and **42**, were obtained from the reaction of **43** with $HGePh_3$.

9) New Highly Active Tin- Containing NanoCatalysts for the Selective Hydrogenations

a) The Hydrogenation of Dimethylterephthalate by using a Platinum-Ruthenium-Tin Precursor Complex.

Thomas et al. have shown that platinum-ruthenium carbonyl cluster complexes can be precursors to high quality bimetallic nanoparticles for catalytic hydrogenations when activated in mesoporous silica. In this project, we have obtained evidence that a combination of the three metals, platinum, ruthenium and tin, provides as yet the best catalyst for the hydrogenation of dimethylterephthalate (DMT) to 1,4-cyclohexanedimethanol (CHD), a valuable reagent for the synthesis of copolymers, see scheme 2.

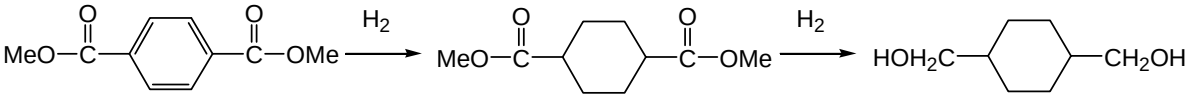

dimethyl terephthalate (DMT) dimethyl hexahydroterephthalate (DMHT) 1,4-cyclohexanedimethanol (CHDM)

Scheme 2

For this work we selected the trimetallic $PtSnRu_5$ cluster complex $PtRu_5(CO)_{15}(\mu\text{-}SnPh_2)(\mu_6\text{-}C)$, **44** that we recently synthesized and reported, see Figure 18. Compound **44** was deposited on mesoporous Davison 38 Å silica. All of the ligands including the phenyl groups on the tin ligand were removed by heating to 200^o C. HAADF TEM images of the silica revealed the presence of nanoparticles 1-2 nm in size. XEDS analysis of individual particles showed that their composition was precisely the same as that of the precursor complex Ru_5PtSn within experimental error. The particles remain small during the catalysis. HAADF TEM images of catalyst particles before and after use for the catalytic hydrogenation of dimethyl terephthalate DMT to cyclohexanedimethanol CHDM are shown in figure 19.

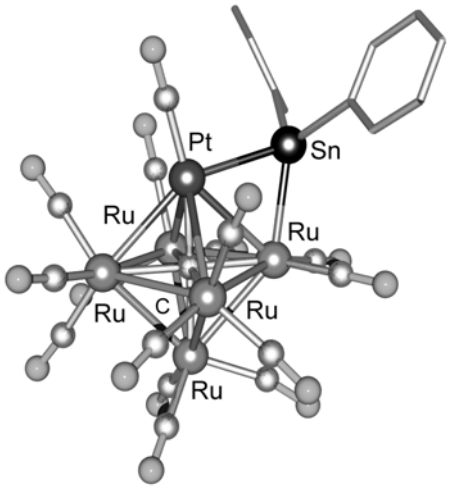

Figure 18. The structure of the molecular cluster $PtRu_5(CO)_{15}(\mu\text{-}SnPh_2)(\mu_6\text{-}C)$, **44**.

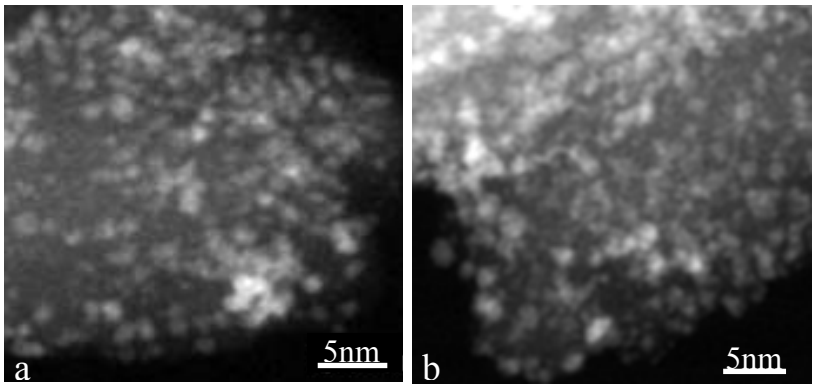

Figure 19. HAADF images of Ru_5PtSn nanoclusters on Davison 38 Å silica (a) before catalysis and (b) after catalysis.

Figure 20 shows a comparison of the activity of some different combinations of metals with ruthenium for the hydrogenation of DMT to CHDM. The trimetallic Ru_5PtSn clearly exhibits the best conversion and best selectivity by far of all the catalysts, Ru_6Sn, Ru_5Pt, Ru_5PtGe and Ru_5PtSn, that were studied and is far superior to the catalysts that are used commercially for this process. Eastman prepares over 200 million pounds of CHDM/year for use in the synthesis of copolyesters by a **two-step** reduction process of DMT.

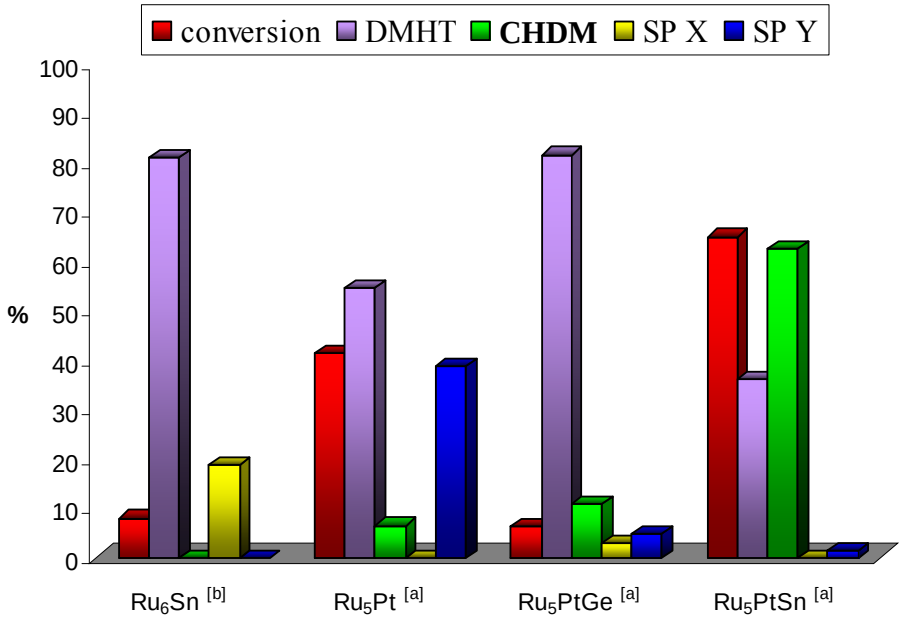

Figure 20. A bar chart comparing the activity and selectivity of the Ru_5PtSn catalyst with other bi-and tri-metallic catalysts for the hydrogenation of dimethylterephthalate.

b) Selective Catalysts for the Hydrogenation of Cyclododecatriene

Cyclododecene (CDE), is a compound of pivotal importance to the chemical industry. It is normally prepared by the selective hydrogenation of 1,5,9-cyclododecatriene (CDT) with metallic Pd being the catalyst of choice to date. But, Pd suffers somewhat from its lack of selectivity, and considerable quantities of the cycloalkane, cyclododecane (CDA) appear as a co-product. It is well known that tin can modify the reactivity of heterogeneous catalysts. It is also known that the homogeneity of the bimetallic cluster catalysts is improved by combining the metals into discrete

bimetallic organometallic complexes prior to deposition on a silica supports and activation by mild thermal treatments, see above. Accordingly, we have have prepared and tested three new tin containing nanoscale catalysts $PtSn_2$, $RhSn_2$ and $RuSn_2$ and compared them with their non-tin containing homologues for the hydrogenation of CDT. For these studies, two new catalyst precursors $(COD)Pt(SnPh_3)_2$, **45** (COD = 1,5-cyclooctadiene) and $Ru(CO)_4(SnPh_3)_2$, **46** have been prepared. For the "$RhSn_2$" catalyst we have used the precursor $Rh_3(CO)_6(SnPh_3)_2(\mu\text{-}SnPh)_2$, **47** (see Fig. 12) the preparation and structure of which were recently reported.

Each of the complexes was deposited from solution on mesoporous silica (Davison type 911 which has mesopores of *ca* 38 Å diameter) and activated by heating to 473 K *in vacuo* for 1h. The nanoscale character of the catalysts and their composition was confirmed by aberration-corrected scanning transmission electron microscopy (STEM) as described previously. For comparison, catalysts derived from pure forms of the PMG catalysts, Pt, Rh and Ru, were also prepared by using supported nanocatalysts thermally derived from the precursors $Pt(COD)_2$, $Rh_4(CO)_{12}$, and $Ru_3(CO)_{12}$, respectively. Images of the $PtSn_2$ and Pt catalysts on the silica support are shown in Figure 21. The bimetallic clusters were shown to be stoichiometric by electron-induced energy dispersive x-ray emission spectroscopy.

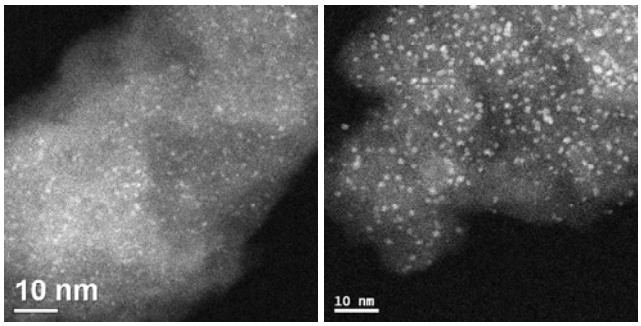

Figure 21. (a) STEM of $PtSn_2$ (left) and Pt (right) nanoclusters on mesoporous silica

The catalytic reactions, (substrate ≅ 50g; catalysts ≅ 25 mg; H_2 pressure ≅ 30 bar, T ≅ 373 K and t ≅ 8h), were performed in a robotically- controlled catalytic test reactor. The results of the catalytic performance of the seven related, supported cluster catalysts are shown in Figure 22.

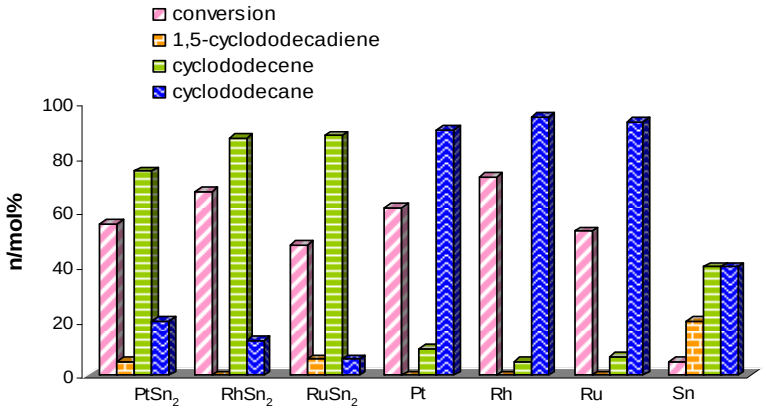

Figure 22. The effect of tin in the selective hydrogenation of 1,5,9-cyclododecatriene (CDT) using anchored monometallic and bimetallic cluster catalysts

The selectivity towards the desired cyclododecene (CDE) is remarkable. Whereas the monometallic catalysts produce almost complete hydrogenation of the CDT to the corresponding alkane, all three bimetallic clusters $RuSn_2$, $RhSn_2$ and $PtSn_2$ exhibit high selectivities towards CDE at approximately the same level of total conversion (50 to 75 percent) of the CDT. Pure tin clusters derived from Ph_2SnH_2 are poor catalysts both in terms of activity and selectivity (conversion less than 10 percent).

In more detailed further studies, we investigated a series of RuSn catalysts derived from cluster complexes obtained form reactions of the tetrahedral tetrahydridotetraruthenium cluster complex $H_4Ru_4(CO)_{12}$ reacts with Ph_3SnH. Four new ruthenium-tin cluster complexes $Ru_4(\mu_4\text{-}SnPh)_2(CO)_{12}$, **48**, $Ru_4(\mu_4\text{-}SnPh)_2(\mu\text{-}SnPh_2)_2(\mu\text{-}CO)_2(CO)_8$, **49**, $Ru_4(\mu_4\text{-}SnPh)_2(\mu\text{-}SnPh_2)_3(\mu\text{-}CO)(CO)_8$, **50**, and $Ru_4(\mu_4\text{-}SnPh)_2(\mu\text{-}SnPh_2)_4(CO)_8$, **51** have been isolated and structurally characterized, see Scheme (3). All four complexes contain two quadruply bridging SnPh stannylyne ligands which produce an octahedral shaped Ru_4Sn_2 cluster and varying numbers of bridging $SnPh_2$ ligands on the edges of the Ru_4 square. All of the hydrido ligands were lost in the formation of **48** and **49** mostly by combining with some of the phenyl groups that were eliminated from Ph_3SnH to form the SnPh ligands. To form **51**, four CO ligands were also replaced by $SnPh_2$ ligands that bridge the each of the four Ru – Ru edges of the Ru_4 square, see Figure 23.

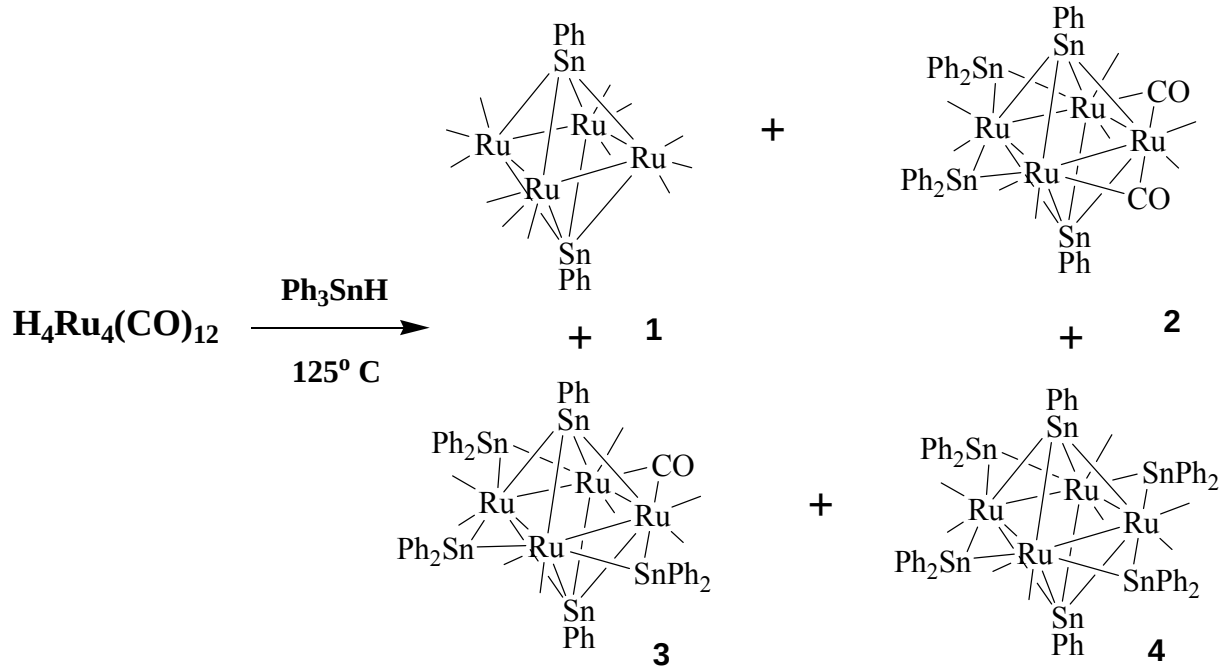

Scheme 3

Compounds **48**, **49** and **51** were chosen for our catalytic investigations. The compounds were deposited (approx. 2% metal loading) on Davison 911 silica mesopore (38 Å) and were activated by heating to 200° C for 2h *in vacuo*.

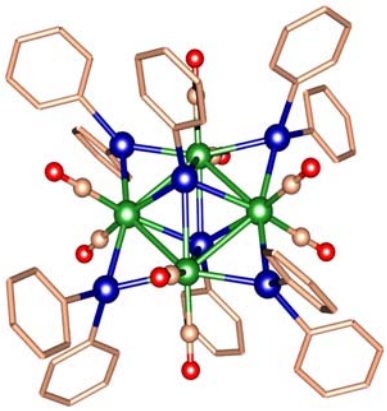

Figure 23. Structural diagram of compound **51**.

The catalysis studies were performed by Professor Robert Raja at the University of Southampton, UK. A comparison of the performance of the two new bimetallic RuSn nanoparticle catalysts with one another and with the Ru_6Sn (chlorine-containing) catalyst is shown in Figure 24. Both in regard to degree of conversion and with respect to selectivity towards formation of the desirable CDE, the Ru_4Sn_6 preparation surpasses the performance of both the Ru_4Sn_2 and Ru_6Sn. It is also noteworthy that, as seen in Figure 24, a substantial increase in conversion (with close to100 percent selectivity) occurs when the reaction is carried out at 413K.

The catalysts were characterized both before and after catalysis by STEM analyses. The metal particles are very small and are uniformly *ca* 1nm in size, allowing for the enlargement in appearance that results from electron optical effects. EDX analysis by SEM shows that the composition of each of the supported catalysts is very similar to the composition of its molecular precursor.

Our results demonstrate not only the superiority of using bimetallic carbonyl complexes as precursors to provide highly dispersed supported naked bimetallic catalysts, but also the beneficial effects of the tin modifier on enhancing the selectivity. There is clearly much scope here to enhance further the catalytic performance of Ru-Sn bimetallic catalysts (by exploring other ratios of Ru:Sn and other structures of precursor entities (from 1:1 to 1:5 of Sn:Ru).

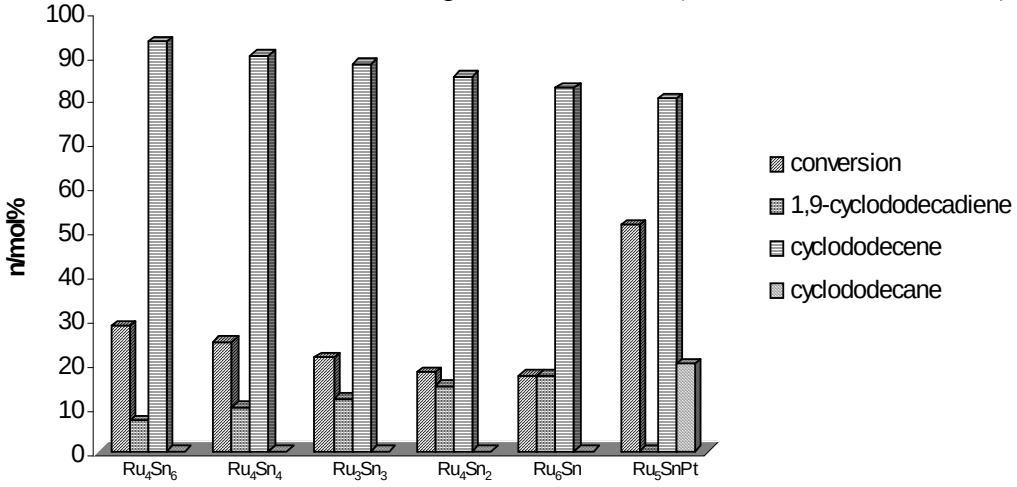

Figure 24. Comparison of catalytic performance of Ru_4Sn_6, Ru_4Sn_4, Ru_4Sn_2 and Ru_5SnPt with the previously reported (chlorine-containing) Ru_6Sn.

b) Michael Amiridis Research Results 2005-2008.

The goal of this project was to prepare heterogeneous catalysts with a well-defined composition of active sites. During the course of this work we have investigated how heterogeneous catalysts can be prepared from Pt clusters in aqueous solutions, as well as how the catalytic properties of Pt can be tailored in the presence of Fe, Ru, and Sn. A summary of the results obtained for each class of investigated materials is provided below.

1. Pt_4 clusters in aqueous solutions as precursors for heterogeneous catalysts.

Preparations of transition metal colloidal suspensions have been known for several years, and metal nanoparticles thus formed have been employed in various fields, such as nanoelectronics, optics, and catalysis. Conventional preparations of colloids involve the reduction of transition metal cations in aqueous solutions. However, the resulting nanoparticles usually are unstable and have a tendency to aggregate and precipitate during the preparation or catalysis. Therefore, various surfactants have to be used to preserve the colloidal state of metal nanoparticles. Such stabilizing agents can strongly interact with the metal nanoparticles and act as poisons, therefore, reducing their catalytic efficiency Our goal was to develop a novel approach for the synthesis of stable and catalytically active Pt colloidal suspensions without the use of any surfactants or protective agents and to evaluate how such colloids can be used for the preparation of highly dispersed supported metal catalysts.

Our preparation technique includes the following steps. An aqueous solution with the concentration of Pt of approximately 2.6×10^{-4} M was prepared from H_2PtCl_6 and was characterized by a pH of 3.3 after aging. The solution was further treated at room temperature under vigorous stirring with a freshly prepared aqueous solution of sodium boronhydride ($NaBH_4$/Pt mass ratio of approximately 3). The EXAFS and UV-Vis results indicate that after the treatment of the H_2PtCl_6 aqueous solution with $NaBH_4$ at room temperature nearly uniform and isolated Pt clusters with nuclearity of 4 were formed. These clusters show a characteristic UV-Vis band at 215 nm and first-shell Pt–Pt contributions with an average coordination number of 3.1 at a bonding distance of 2.71 Å. The analysis of the XANES region of the EXAFS spectrum indicates that such a treatment was accompanied by a substantial reduction of the white line area value, which is consistent with the reduction of the Pt^{4+} cations to a zerovalent state. The resulting colloidal suspension of "naked" Pt clusters was stable at room temperature for at least 18 months and did not precipitate even in the presence of air.

The catalytic activity of these "naked" Pt clusters was evaluated for the liquid phase selective oxidation of 2-propanol to acetone in the presence of air. UV-Vis and EXAFS data indicate that the Pt clusters tend to nucleate further after the addition of 2-propanol to the solution, probably due to a change of the surface charge of Pt clusters, which leads to the formation of larger Pt nanoparticles with an average Pt–Pt coordination number of 7.4 at a bonding distance of 2.75 Å. Even though some aggregation of the metal took places during this step, the Pt nanoparticles remained stable in the solution and did not precipitate, likely due to the presence of 2-propanol, acting as a stabilizing agent. These Pt nanoparticles are active for the selective oxidation of 2-propanol, as evidenced by the appearance of acetone in the solution when air is passed through. The data indicate that this is a first order reaction in respect to 2-propanol and complete conversion of 2-propanol to acetone was obtained after 4 h. *In-situ* EXAFS data indicate that

under reaction conditions Pt nanoparticles remained in a reduced state, as evidenced by the white line area of the spectra. However, the average Pt–Pt coordination number was gradually increased during first the 60 minutes of the reaction from 7.4 to 8.8 and did not changed thereafter, consistent with further nucleation of Pt nanoparticles during the initial stages of the reaction. However, the final solution did not show any evidences of the precipitation, demonstrating a high stability of formed Pt nanoparticles.

We have further shown that "naked" Pt clusters with nuclearity of 4, initially formed in a solution can be delivered on a γ-Al_2O_3 support surface by lowering the pH from 7.0 to approximately 2.0. EXAFS data indicate that after the deposition and drying, the supported Pt species formed have structures very similar to those of the corresponding colloidal suspensions. This Pt_4/γ-Al_2O_3 sample was found to be active for the oxidation of CO without any need for additional activation. Nevertheless, treatment of this sample with H_2 in the 150-200°C temperature range leads to the formation of Pt aggregates with sizes on the order of 1.0 to 1.6 nm, demonstrating that platinum readily sinters under reducing conditions.

2. Structure and reactivity of cluster-derived $PtFe/SiO_2$ catalysts.

The goal of this work was to prepare and characterize SiO_2-supported Pt–Fe catalysts from $Pt_5Fe_2(COD)_2(CO)_{12}$ and $PtFe_2(COD)(CO)_8$, precursors which already contain well-defined Pt–Fe bonds. Such supported catalysts were prepared by mixing of the $Pt_5Fe_2(COD)_2(CO)_{12}$ or $PtFe_2(COD)(CO)_8$ precursors in CH_2Cl_2 with the powdered SiO_2 support in a slurry for 24 h under nitrogen flow in the absence of light. The solvent was allowed to evaporate slowly during this period to ensure complete uptake of the precursor by the support. The amount of each precursor was chosen to yield samples containing 1 wt% Pt after ligand removal. The corresponding Fe content was 0.57 and 0.11 wt % for $PtFe_2(COD)(CO)_8/SiO_2$ and $Pt_5Fe_2(COD)_2(CO)_{12}/SiO_2$, respectively. Monometallic Pt/SiO_2 and bimetallic $PtFe/SiO_2$ samples with different Pt/Fe ratios were also prepared for comparison by conventional incipient wetness impregnation of the support with an aqueous solution of H_2PtCl_6 and appropriate mixtures of H_2PtCl_6 and $Fe(NO_3)_3$, respectively.

EXAFS and IR spectroscopy were used to characterize the surface species formed following the interaction of $Pt_5Fe_2(COD)_2(CO)_{12}$ and $PtFe_2(COD)(CO)_8$ with SiO_2 and to monitor the decarbonylation process needed to activate these catalysts. The results indicate that both clusters can be deposited intact on the SiO_2 support. Both clusters remained weakly bonded to the support and could be extracted from the surface back into a CH_2Cl_2 solution without any significant changes in their structure. Infrared data further indicate that subsequent heating in H_2 or He led to a gradual removal of the ligands, a process that was completed at approximately 350°C. The treatment in H_2 appeared to be more favorable than that in He. For example, when $Pt_5Fe_2(COD)_2(CO)_{12}$ was used as the precursor, the Pt atoms remained mostly bonded to Fe atoms after removal of the ligands in H_2, as evidenced by first-shell Pt–Fe contributions with a coordination numbers of 1.0 at a bond distance of 2.67 Å (measured at the Pt L_3 edge) and first-shell Fe–Pt contributions with a coordination number of 2.3 at a distance of 2.67 Å (measured at the Fe *K* edge). Thus, the EXAFS results suggest that the Pt–Fe interactions were strong in this case and were largely maintained during decarbonylation under reducing conditions, although the geometry of the cluster frame was changed significantly, as indicated by a change in the average Pt–Pt and Pt-Fe bond distances. In contrast, the He treatment appears to lead to complete disintegration of the cluster frame. IR results further indicate that the original cluster

can not be reconstructed by exposure of the decarbonylated species to CO, thus demonstrating the irreversible character of the structural changes taking place during removal of the ligands. The observed structural changes during removal of the ligands were also accompanied by an increase of the Pt–Pt fist-shell coordination number from 3.2 to 6.0, indicating some aggregation of Pt. However, the degree of such aggregation was relatively low, resulting in the formation of PtFe bimetallic nanoparticles with an average size below 1 nm. The formation of such nanoparticles is likely the result of the nucleation of Pt_5Fe_2 units, since the atomic Pt/Fe ratio in them (estimated from EDX data) is similar to the 2.5 ratio in the original $Pt_5Fe_2(COD)_2(CO)_{12}$ cluster precursor. A $PtFe/SiO_2$ reference sample prepared by co-impregnation from monometallic Pt and Fe precursors and treated in H_2 at 350°C also exhibited some bimetallic character, but was less dispersed than the cluster-derived sample and exhibited a higher degree of segregation between the two metals.

Adsorption of probe molecules (i.e., CO and NO) on the different bimetallic samples indicates the presence of electron rich Pt sites. The formation of these sites can be attributed to electronic interactions between Pt and Fe atoms, which are maximized when the $Pt_5Fe_2(COD)_2(CO)_{12}$ cluster is used as a precursor. Moreover, the infrared data indicate that Fe in these bimetallic samples is present in both the $Fe^{\delta+}$ and Fe^0 forms, suggesting that Pt facilitates the reduction of Fe. The fraction of fully reduced Fe sites was greater in the Pt_5Fe_2/SiO_2 sample characterized by the largest fraction of Pt–Fe interactions, implying that close proximity between the two metals is an important factor affecting the reduction process. Furthermore, hydrogen chemisorption data indicate a strong reduction of the chemisorptive properties in the samples with the greater number of Pt–Fe interactions. The strength of CO adsorption on these bimetallic samples also appeared to be following a similar pattern.

Kinetic data for the oxidation of CO in air show that both the Pt_5Fe_2/SiO_2 and $PtFe_2/SiO_2$ samples were more active for this reaction than Pt/SiO_2. The effect was more pronounced when the $Pt_5Fe_2(COD)_2(CO)_{12}$ cluster was used as the precursor. This sample showed a significant conversion of CO even at room temperature, although it deactivates with time on stream, indicating that the Pt–Fe bimetallic sites that presumably yield the enhanced reaction rate are sensitive to the reaction conditions. The Pt_5Fe_2/SiO_2 sample also exhibited superior activity to that of Pt/SiO_2 for the selective oxidation of CO under H_2-rich conditions. In addition to the high activity for this reaction, the Pt_2Fe_5/SiO_2 sample exhibited a selectivity of approximately 92% at temperatures up to 60°C, indicating that the competitive reaction of H_2 oxidation was substantially suppressed in this case. The enhancement of the catalytic activity for both reactions and the high selectivity in PROX could be related to the formation of PtFe bimetallic sites on the SiO_2 surface, in which Pt atoms are directly bonded to Fe^{n+} ions or reduced Fe^0 atoms.

3. Investigation of $PtFe/SiO_2$ catalysts prepared by coimpregnation.

Even though these cluster-derived Pt–Fe catalysts have relatively simple and uniform structures, the fixed composition of heterometallic cluster precursors substantially limits the range in which the effect of the metal composition on the structure and the catalytic performance can be evaluated and does not allow us to estimate the optimal content of Fe in the formulation. Therefore, to broaden the range in which the effect of Fe on the catalytic properties of SiO_2-supported Pt can be evaluated, a family of $PtFe/SiO_2$ samples with different Pt/Fe ratios was prepared from individual H_2PtCl_6 and $Fe(NO_3)_3$ precursors and characterized by hydrogen chemisorption, EXAFS and FTIR measurements. These characterization results were further

combined with kinetic data obtained for reactions taking place in both oxidative and reducing environments (such as the oxidation of CO, the dehydrogenation of cyclohexane, and the selective hydrogenation of citral) to derive conclusions regarding the role of each metal during catalysis, as well as structure-reactivity correlations for the bimetallic Pt–Fe system.

HRTEM results showed that the treatment of these samples with H_2 at 350°C leads to the formation of metal particles with sizes on the order of 2.6 nm, while both EDX and EXAFS data suggest that some of these particles are bimetallic in nature and likely exhibit raft-type geometry. It was also shown by EXAFS that the fraction of bimetallic Pt–Fe interactions in each sample strongly depends on the composition and decreases with increasing Fe content, suggesting that Fe does not only interact with Pt but also forms an oxide-like species. Results of CO and NO adsorption FTIR measurements on these bimetallic samples provide evidence for the presence of electronic interactions between Pt and Fe, resulting in the formation of electron-rich Pt sites. The extent of electron density transfer between Fe and Pt depends on the composition and decreases with increasing content of Fe. Moreover, the FTIR results indicate that Fe in these bimetallic samples is present in both the $Fe^{\delta+}$ and Fe^0 forms, suggesting that Pt - being in close proximity to Fe - facilitates the reduction of Fe to the metallic state. In addition, chemisorption results indicated that both the chemisorption of hydrogen and the strength of CO adsorption on Pt are also affected significantly by the amount of Fe present. Therefore, this comprehensive investigation of a family of bimetallic $PtFe/SiO_2$ samples suggests that the structure, electronic, and chemisorptive properties of Pt are modified substantially in the presence of Fe, providing an opportunity to evaluate the effect of these properties on the catalytic performance of Pt for different reactions.

The kinetic results obtained for the different $PtFe/SiO_2$ catalysts for all three reactions examined indicate that the catalytic behavior of Pt is affected significantly by the presence of Fe. $PtFe/SiO_2$ samples for example, were found to be more active than monometallic Pt/SiO_2 for the oxidation of CO in air. This enhancement of the catalytic activity strongly depends on the fraction of Pt–Fe interactions in the different catalysts, the degree of electronic interaction between the metals, and the strength of CO adsorption. Similarly, the addition of Fe to Pt/SiO_2 in small concentrations promotes the activity of Pt for the dehydrogenation of cyclohexane and the selective hydrogenation of citral, which can be attributed to an electronic effect and/or the presence of bimetallic Pt–Fe sites. The close proximity between Pt and Fe in such sites leads to the reduction of Fe, which can be active for cyclohexane dehydrogenation. Furthermore, Pt–Fe adsorption sites could favor the di-σ_{CO} mode of adsorption for α,β-unsaturated aldehydes, thus promoting the selective hydrogenation of the C=O bond and the formation of α,β-unsaturated alcohols. In both cases however, the presence of large amounts of Fe leads to eventual deactivation of Pt, most probably due to the formation of an iron oxide phase.

4. Kinetic characterization of multimetallic cluster-derived catalysts.

Cluster-derived multimetallic supported catalysts have been also investigated using the selective hydrogenation of citral as a probe reaction. The catalysts examined included supported multimetallic clusters containing combinations of Pt, Ru, and Sn, as well as samples of identical compositions prepared by impregnation from individual salt precursors on various oxide supports. The clusters of interest involve combinations of Pt, Ru, and Sn. For the synthesis of these clusters, the parent molecule (i.e., $Ru_5(CO)_{15}(\mu_5\text{-}C)$) was reacted with $Pt(COD)Cl_2$ and/or Ph_3SnH to form $Ru_5(SnPh_3)(C)(CO)_{15}$, $PtRu_5(C)(CO)_{16}$, $Pt(SnPh_3)_2(COD)$, and $PtRu_5(\mu$-

$SnPh_2)(C)(CO)_{15}$ clusters, which were subsequently used as precursors for the preparation of supported heterogeneous catalysts.

Kinetic data for the hydrogenation of citral were collected at 70C in a stirred autoclave reactor under a hydrogen pressure of 460psig. Samples were analyzed by GC to determine the conversion and selectivity to the α,β-unsaturated alcohols (i.e. geraniol and nerol). Catalyst mesh size, autoclave stir rate, and the amount of catalyst were varied independently to study mass transfer effects and to insure that no internal or external mass transport limitations were present in the reactor set-up employed. The kinetic results obtained indicate that the trimetallic cluster-derived catalyst, $PtRu_5Sn$, exhibited enhanced activity and selectivity over the various bimetallic cluster-derived and all metal salt-impregnated catalysts. Presumably the addition of Sn to the Pt-Ru cluster-derived system stabilizes the resulting supported moieties and modifies the catalytic properties of Pt and Ru, directly affecting overall activity and selectivity to the α,β-unsaturated alcohols. Conversely, the addition of Sn to the coimpregnated Pt-Ru samples does not substantially change their catalytic performance when compared to the cluster-derived trimetallic catalyst.

Furthermore, in the case of the trimetallic cluster precursor, the use of MgO as a support more than doubled the reaction rate and selectivity to the α,β-unsaturated alcohols when compared to less basic silica and alumina supports. This result suggests that increasing the overall basicity decreases the probability of conjugated C=C double bond hydrogenation, while simultaneously rendering the hydrogenation of the aldehyde group more thermodynamically favorable. For the $PtRu_5Sn$ cluster-derived catalyst, the use of MgO as a support appears to enhance the effect of the electron donating properties of the Sn promoter. Some degree of deactivation was observed for the alumina and silica supported catalysts, presumably due to agglomeration of the catalyst particles on these supports. No such deactivation was observed for the MgO support.

HRTEM measurements indicate that the metal particle size for the cluster-derived catalysts is smaller (1.0-1.2 nm) than the corresponding particle size for the salt-derived ones (1.0-5.4 nm). EDX spot analysis performed on these samples further shows that the $PtRu_5Sn$ cluster-derived catalyst particles have a consistent composition, analogous to the cluster precursor. However, the Pt-Ru-Sn in the salt-derived catalysts particles vary greatly in composition, and the presence of several large Pt and Ru particles indicates agglomeration on the support. When comparing the kinetic data and HRTEM/EDX results, the presence of these metals in close proximity appears to greatly enhance selectivity and activity for the cluster-derived catalysts. Therefore, the use of bimetallic and trimetallic organometallic cluster precursors can yield better-defined and more uniform catalysts with distinct advantages over their analogous metal salt precursors.

C) Publications for this Project for the Years 2005 - 2008.

1) Richard D. Adams Publications

1) R. D. Adams, B. Captain, M. Johansson, and J. L. Smith, Jr., New Rhenium-Tin Cluster adds Palladium Phosphine Groups across Re-Sn Bonds, *J. Am. Chem. Soc.* **2005**, *127*, 488.
2) R. D. Adams, B. Captain, M. B. Hall, J. L. Smith, Jr., and C. E. Webster, High Nuclearity Iridium-Platinum Clusters: Syntheses, Structures, Bonding, and Reactivity, *J. Am. Chem. Soc.* **2005**, *127*, 1007.
3) R. D. Adams, B. Captain, and J. L. Smith, Jr., High-Nuclearity Iridium Carbonyl Clusters Containing Phenylgermyl Ligands - Synthesis, Structure, and Reactivity, *Inorg. Chem.*, **2005**, *44*, 1413.
4) R. D. Adams, B. Captain, Highly Unsaturated Platinum-Rhenium Cluster Complex Adds an Unusually Large Amount of Hydrogen, *Angew. Chem. int. Ed.*, **2005**, *44*, 2531.
5) R. D. Adams, B. Captain and L. Zhu, New High Nuclearity Platinum-Ruthenium Carbonyl Cluster Complexes Containing a Phenylacetylene Ligand: Structures and Properties, *Organometallics*, **2005**, *24*, 2419.
6) R. D. Adams, B. Captain, and J. L. Smith, Jr. Rhodium Cluster Complexes Containing Bridging Phenylgermyl Ligands, *Inorg. Chem.*, **2005**, *44*, 4276.
7) R. D. Adams, B. Captain, R. H. Herber, M. Johansson, I. Nowik, J. L. Smith, Jr. and M. D. Smith, Addition of Palladium and Platinum Tri-*tert*-Butylphosphine Groups to Re–Sn and Re–Ge Bonds, *Inorg. Chem.,* **2005**, *44*, 6346.
8) R. D. Adams and J. L. Smith, Jr., Rhenium Carbonyl Complexes Containing Bridging $SiPh_3$ and $SiPh_2$ Ligands, *Organometallics*, **2005** *24*, 4489.
9) R. D. Adams, B. Captain and L. Zhu, Synthesis of $PtRu_5(CO)_{14}(PBu^t_3)(\mu\text{-}H)_2(\mu_6\text{-}C)$ and its Reactions with $Pt(PBu^t_3)_2$, $HGePh_3$, and $HSnPh_3$, *Inorg. Chem.*, **2005**, *44*, 6623.
10) R. D. Adams, B. Captain and L. Zhu, Addition of Alkynes to High Nuclearity Platinum-Ruthenium Carbonyl Cluster Complexes, *J. Cluster Sci.,* **2005**, *16*, 397.
11) R. D. Adams, B. Captain, W. Fu, M. D. Smith and L. Zhu, Platinum-Osmium Cluster Complexes from the Addition of $Pt(PBu^t_3)$ groups to $Os_3(CO)_{12}$, *Inorg. Chem.*, **2006**, *45*, 430.
12) R. D. Adams, B. Captain and L. Zhu, $Pd(PBut_3)$ Adducts of $Os_3(CO)_{12}$. Synthesis and Structures of $Pd_2Os_3(CO)_{12}(PBut_3)_2$ and $Pd_3Os_3(CO)_{12}(PBut_3)_3$, *J. Cluster Sci.,* **2006**, *17*, 87-95.
13) R. D. Adams, B. Captain, W. Fu, M. D. Smith, New Highly Unsaturated Platinum – Rhenium Cluster Complex Activates Hydrogen Reversibly Under Mild Conditions, *Angew. Chem. int. Ed.*, **2006**, *45*, 1109-1112.
14) R. D. Adams, B. Captain and L. Zhu, The Importance of Cluster Fragmentation in the Catalytic Hydrogenation of Phenylacetylene by $PtRu_5$ Carbonyl Cluster Complexes, *J. Organomet. Chem*., **2006**, *691*, 3122-3128.
15) A. Siani, B. Captain, O. S. Alexeev, E. Stafyla, A. B. Hungria, P. A. Midgley, J. M. Thomas, R. D. Adams, M. D. Amiridis, Improved CO Oxidation Activity in the Presence and Absence of Hydrogen over Cluster derived $PtFe/SiO_2$ Catalysts, *Langmuir*, **2006**, *22*, 5160-5167.

16) R. D. Adams, B. Captain and L.Zhu, A New Tris-(diphenylstannylene)triosmium Carbonyl Cluster Complex and its Reactions with $Pt(PBu^t_3)_2$ and $Pt(PPh_3)_4$, *Organometallics*, **2006**, *25*, 2049-2054.
17) A. B. Hungria, R. Raja, R. D. Adams, B. Captain, J. M. Thomas, P. A. Midgley, V. Golvenko and B. F. G. Johnson, Single-Step Conversion of Dimethyl Terephthalate to Cyclohexanedimethanol with A Trimetallic Nanoparticle Catalyst: Ru_5PtSn, *Angew. Chem. int. Ed.*, **2006**, *45*, 4782-4785.
18) R. D. Adams, C. B. Hollandsworth and J. L. Smith, Jr., Unsaturated Cyclopentadienyl-Molybdenum and Tungsten Carbonyl Cluster Complexes Containing Pd- and $Pt(PBu^t_3)$ Groups, *Organometallics*, **2006**, *25*, 2673-2682.
19) R. D. Adams, B. Captain, C. B. Hollandsworth, M. Johansson, J. L. Smith, Jr., Synthesis and Structures of Oxo-Bridged Distannyl- and Digermyldirhenium Complexes, *Organometallics*, **2006**, *25*, 3848-3855.
20) R. D. Adams, B. Captain and L.Zhu, Cluster Fragmentation and Facile Cleavage of Phenyl groups from the $SnPh_3$ Ligand in Reactions of $Os_3(CO)_{11}(SnPh_3)(\mu\text{-}H)$ with CO and $HSnPh_3$, *Organometallics*, **2006**, *25*, 4183-4187.
21) R. D. Adams, B. Captain, W. C. Pearl, Jr., Bimetallic Clusters of Iron with Palladium and Platinum. Synthesis and Structures of $Fe_2(CO)_9[M(PBu^t_3)]_2$ (M = Pd or Pt) and $Fe_2(CO)_8[Pt(PBu^t_3)]_2(\mu\text{-}H)_2$, *Inorg. Chem.*, **2006**, *45*, 8283-8287.
22) R. D. Adams, B. Captain and L.Zhu, Platinum Promoted Insertion of an Alkyne into a Metal-Hydrogen Bond, *J. Am. Chem. Soc.* **2006**, *128*, 13672-13673.
23) B. L. García, B. Captain, R. D. Adams, A. B. Hungria, P. A. Midgley, J. M. Thomas and J. W. Weidner, Bimetallic Cluster Provides a High Activity Electrocatalyst for Methanol Oxidation, *J. Cluster Sci.,* **2007**, *18*, 121-130.\
24) R. D. Adams, B. Captain, C. Beddie and M. B. Hall, Photo-reversible Multiple Additions of Hydrogen to a Highly Unsaturated Platinum-Rhenium Cluster Complex, *J. Am. Chem. Soc.,* **2007**, *129*, 986-1000.
25) R. D. Adams, E. M. Boswell, B. Captain, and M. A. Patel, Multiple Additions of Phenylgermanium Ligands to Tetraruthenium and Tetraosmium Carbonyl Cluster Complexes, *Inorg. Chem.* **2007**, *46*, 533-540.
26) R. D. Adams, B. Captain and L.Zhu, Facile Activation of Hydrogen by an Unsaturated Platinum-Osmium Cluster Complex, *J. Am. Chem. Soc.* **2007**, *129*, 2454-2455.
27) R. D. Adams, B. Captain, Mark D. Smith, C. Beddie and M. B. Hall, Unsaturated Platinum-Rhenium Cluster Complexes. Synthesis, Structures and Reactivity, *J. Am. Chem. Soc.* **2007**, *129*, 5981-5991.
28) R. D. Adams, B. Captain, E. Trufan and L. Zhu, The Activation of Metal Hydride Complexes by Tri-t-butylphosphine-Platinum and -Palladium Groups, *J. Am. Chem. Soc.* **2007**, *129*, 7545-7556.
29) R. D. Adams, B. Captain and L.Zhu, The Addition of $Pt(PBu^t_3)$ to Osmium-Tin Cluster Complexes, *Inorg. Chem.* **2007**, *46*, 4605-4611.
30) R. D. Adams and B. Captain, Saturated vs. Unsaturated: Ligand Addition to the Saturated Metal Site of an Unsaturated Binuclear Metal Complex, *Angew. Chem.. int. Ed.* **2007**, *46*, 5714-5716.
31) R. D. Adams, B. Captain, and E. Trufan, Ruthenium carbonyl cluster complexes with phenylgermyl ligands from the reactions of Ph_3GeH with $Ru(CO)_5$ and $Ru_3(CO)_{12}$, *J. Cluster Sci.* **2007**, *18*, 642-659.

32) R. D. Adams, E. M. Boswell, B. Captain, A. B. Hungria, P. A. Midgley, R. Raja, J. M. Thomas, Bimetallic Ru-Sn Nanoparticle Catalysts for the Solvent-free, Selective Hydrogenation of 1,5,9-Cyclododecatriene to Cyclododecene, *Angew. Chem.. int. Ed.,* **2007**, *46*, 8182-8185.
33) R. D. Adams, B. Captain, M. B. Hall, E. Trufan, and X. Yang, The Synthesis, Characterization and Electronic Structures of a Novel Series of 2-Dimensional Trimetallic Cluster Complexes, $Ru_3(CO)_9(\mu\text{-}SnPh_2)_3[Pt(PBu^t_3)]_x$, x = 0 – 3, *J. Am. Chem. Soc.,* **2007**, *129,* 12328-12340.
34) R. D. Adams, B. Captain and P. J. Pellechia, Studies of Ligand Additions to Coordinatively Unsaturated Dirhenium Complexes Containing the bulky PBu^t_3 Ligand, *Organometallics,* **2007**, *26*, 6564-6575.
35) R. D. Adams, B. Captain and L.Zhu, Facile Activation of Hydrogen by Unsaturated Platinum-Osmium Carbonyl Cluster Complexes, *J. Organomet. Chem.,* **2008**, *693*, 819-833.
36) R. D. Adams, E. M. Boswell, B. Captain, and L. Zhu, Platinum-Ruthenium Cluster Complexes from the Reaction of $Ru_3(CO)_{12}$ with $Pt(PBu^t_3)_2$, *J.Cluster Sci.,* **2008**, *19*, 121-132.
37) R. D. Adams, E. Boswell, and B. Captain, Synthesis and Properties of an Unusual New High Symmetry Osmium-Palladium Carbonyl Cluster Complex, *Organometallics*, **2008**, *27*, 1169-1173.
38) R. D. Adams, B. Captain, W. C. Pearl, Jr., Facile Cleavage of a Phenyl Group from $SbPh_3$ by Dirhenium Carbonyl Complexes, *J. Organomet. Chem.* **2008**, *693*, 1636-1644.
39) R. D. Adams, E. Boswell, Cleavage of t-butyl Groups from the Tri-t-butylphosphine Ligand in Osmium-Platinum Carbonyl Cluster Complexes, *Organometallics*, **2008**, *27*, 2021-2029.
40) R. D. Adams, D. A. Blom, B. Captain, R. Raja, J. M. Thomas, and E. Trufan, Toward Less Dependence on Platinum Group Metal Catalysts: The Merits of Utilizing Tin, *Langmuir,* **2008**, *24*, 9223-9226.

2) Michael D. Amiridis Publications

1) A. Siani, O. S. Alexeev, G. Lafaye, P. Marecot, M. D. Amiridis. "The effect of Fe on SiO_2-supported platinum catalysts: I. Structure and chemisorptive properties", *J. Catal.* (2008), submitted.
2) A. Siani, O. S. Alexeev, G. Lafaye, P. Marecot, M. D. Amiridis. "The effect of Fe on SiO_2-supported platinum catalysts: II. Catalytic activity", *J. Catal.* (2008), submitted.
3) A. Siani, K. R. Wigal, O. S. Alexeev, M. D. Amiridis. "Synthesis and characterization of Pt clusters in aqueous solutions", *J. Catalysis* 257 (2008) 5.
4) A. Siani, K. R. Wigal, O. S. Alexeev, M. D. Amiridis. "Synthesis and characterization of γ-Al_2O_3-supported Pt catalysts from Pt_4 and Pt_6 clusters formed in aqueous solutions", *J. Catal.* 257 (2008) 16.
5) A. Siani, O. S. Alexeev, B. Captain, G. Lafaye, P. Marecot, R. D. Adams, M. D. Amiridis. "Synthesis of cluster-derived $PtFe/SiO_2$ catalysts for the oxidation of CO", *J. Catal.* 255 (2008) 162.

6) A. Siani, B. Captain, O. S. Alexeev, E. Stafyla, A. B. Hungria, J. M. Thomas, R. D. Adams, M. D. Amiridis. “Improved CO oxidation activity in the presence and absence of hydrogen over cluster-derived $PtFe/SiO_2$ catalysts”, *Langmuir* 22 (2006) 5160.
7) O.S. Alexeev, F. Li, M.D. Amiridis, and B.C. Gates, "Effects of Adsorbates on Supported Platinum and Iridium Clusters: Characterization in Reactive Atmospheres and During Alkene Hydrogenation Catalysis by X-Ray Absorption Spectroscopy ", *J. Phys. Chem. B*, 109(6), 2338-2349, (2005).
8) O.S. Alexeev, S.Y. Chin, M.H. Engelhard, L.B. Ortiz-Soto, and M.D. Amiridis, "Effects of Reduction Temperature and Metal-Support Interactions on the Catalytic Activity of Pt/γ-Al_2O_3 and Pt/TiO_2 for the Oxidation of CO in the Presence and Absence of H_2", *J. Phys.l Chem. B*, **109(49)**, 23430-23443, (2005).